water

MDPI

Article

Environmentally Sensitive Elements in Groundwater of an Industrial Town in India: Spatial Distribution and Human Health Risk

Dapinder Deep Singh [1], Parteek Singh Thind [2], Mukta Sharma [3], Sashikanta Sahoo [4] and Siby John [2,*]

1 Department of Civil Engineering, IK Gujral Punjab Technical University, Kapurthala 144601, India; dapinder1111@gmail.com
2 Department of Civil Engineering, Punjab Engineering College, Chandigarh 160012, India; prateek.thind@gmail.com
3 Department of Geology, School of Built Environment, IK Gujral Punjab Technical University, Kapurthala 144601, India; muktageo@gmail.com
4 Geology, Water Resources and Geoinformatics Division, Punjab Remote Sensing Centre, Ludhiana 141004, India; sksahoo@prsc.gov.in
* Correspondence: johnsiby1@gmail.com; Tel.: +91-94634-95575

Received: 22 September 2019; Accepted: 5 November 2019; Published: 8 November 2019

Abstract: This paper presents the results of a study to assess the groundwater quality in an industrial town located in Punjab, India. A total of 99 samples of groundwater were analyzed during the premonsoon and postmonsoon periods of 2018, which revealed the presence of numerous environmentally sensitive elements (ESEs), namely, arsenic (As), aluminum (Al), chromium (Cr), iron (Fe), mercury (Hg), nickel (Ni), selenium (Se), and lead (Pb). Geographic information system (GIS)-based spatial interpolation showed higher contamination levels around the industrial areas and the drainage channel where industrial effluent is generally discharged. Further, groundwater quality was assessed using the heavy metal pollution index (HPI) and the metal index (MI), which indicated poor drinkability of the groundwater. Human exposure to groundwater contaminated with ESEs can pose serious health risks; therefore, noncarcinogenic and carcinogenic health risks due to presence of these elements were also evaluated. Reported health risks to humans from exposure to contaminated groundwater indicate the importance of regular monitoring of groundwater for ESEs vis-a-vis industrial effluent disposal practices.

Keywords: environmentally sensitive elements; groundwater quality; GIS; health risk assessment; heavy metal pollution index; metal index

1. Introduction

Groundwater is a key natural resource which serves the drinking, agricultural, and industrial needs of one-third of the human population [1,2]. In recent years, the diminishing quantity and degraded quality of surface water bodies have substantially increased the burden on earth's groundwater [3]. Activities such as mining, dumping of solid biomass in landfills, leaching of agrochemicals, and improper disposal of industrial effluents have contaminated the groundwater with various environmentally sensitive elements (ESEs), such as heavy metals, arsenic, pesticides, fertilizers, and so forth. [4]. Groundwater quality is a major concern in both developed and developing nations [5]. Several studies from various parts of the world have highlighted the issue of deteriorating groundwater quality in Bangladesh [6], China [7], South Africa [8], Iran [9], Italy [10], Korea [11], Pakistan [12], and Thailand [13]. Some of these studies have also indicated public health issues arising out of human exposure to contaminated

groundwater. In India, groundwater serves 85%, 50%, and 60% of the drinking, urban water use, and irrigation needs, respectively [14]. Owing to potential cumulative toxicity and persistence, contamination of groundwater with heavy metals has become a focus area for researchers in various states of India, such as Andhra Pradesh [15], Chandigarh [16], Goa [17], Punjab [18], Rajasthan [19], Tamilnadu [20], Uttrakhand [1], and Uttar Pardesh [21]. Geogenic sources, rapid urbanization, unplanned and improper industrial waste disposal, agricultural practices, and so forth, have been identified as the major causes of groundwater contamination [22–24]. Continuous exposure to different heavy metals through water may pose toxicological problems in human beings [25–27].

Ludhiana, Punjab, India is a fast-growing industrial hub. The indiscriminate disposal of domestic, agricultural, and industrial waste in the area poses a potential threat to its groundwater [28]. However, no comprehensive evaluation of the groundwater pollution caused by ESEs such as heavy metals and arsenic and its associated health risk assessment has been conducted in the area.

Keeping this in view, the present study focused on a comprehensive evaluation of ESEs in the groundwater of Ludhiana, Punjab, India during pre- and postmonsoon periods of 2018 (the postmonsoon period was defined as 1–2 months after the monsoon). The objectives of the study were (1) to assess the concentration of ESEs, namely, As, Al, Cr, Fe, Hg, Ni, Se, and Pb, in groundwater; (2) to compare the variation in concentration of the ESEs in groundwater during pre- and postmonsoon periods; (3) to determine the geospatial variation of ESEs and their statistical source apportionment during pre- and postmonsoon periods; (4) to identify the major hotspots by using pollution assessment index approaches, such as the heavy metal pollution index (HPI) and the metal index (MI); and (5) to evaluate the possible human health risks due to exposure to ESE-contaminated groundwater in terms of noncarcinogenic and carcinogenic effects through ingestion and dermal pathways. Statistical analysis of the findings of the field study helped to deduce the inferences. The geographic information system (GIS) was used to present the geospatial variation of the ESEs. The findings of this study should attract the attention of pollution control agencies and policy makers towards the degrading groundwater quality of the region and emphasize the need of establishing stringent policies to reduce the groundwater contamination.

2. Materials and Methods

2.1. Study Area Description

The Ludhiana district of Punjab, India, which is one of the industrial hubs of North India, was the study area. Figure 1 shows the geographical location, landuse, landcover, and the sampling locations of the study area. Sutlej River flows along its northern boundary. The entire geographical area is 3767 km^2 and has 3.5 million human inhabitants [29]. The mean annual rainfall is about 577 mm [30]. The mean maximum and minimum temperatures are 45 and 6 °C in the months of June and December, respectively [31]. The major water requirements of the area are for agricultural, domestic, and industrial demands. Groundwater, rainwater, and canal water are used to meet the agrarian needs; however, the domestic and industrial demands are met with groundwater sources only. Major industries located in the study area include micro, small, medium, and large businesses of different types, namely, chemicals, fabricated metals, bicycle and bicycle parts, machine tools, rubber goods, hosiery goods, beverages, textiles, dyeing, paper products, and electroplating. There are 37,047 (micro, small, and medium) businesses and 151 large-scale businesses which are registered in the study area [32]. Studies have reported increasing groundwater quality deterioration in the study area due to activities such as industrial wastewater disposal, disposal of garbage, use of fertilizers, and pesticides on agricultural land [28].

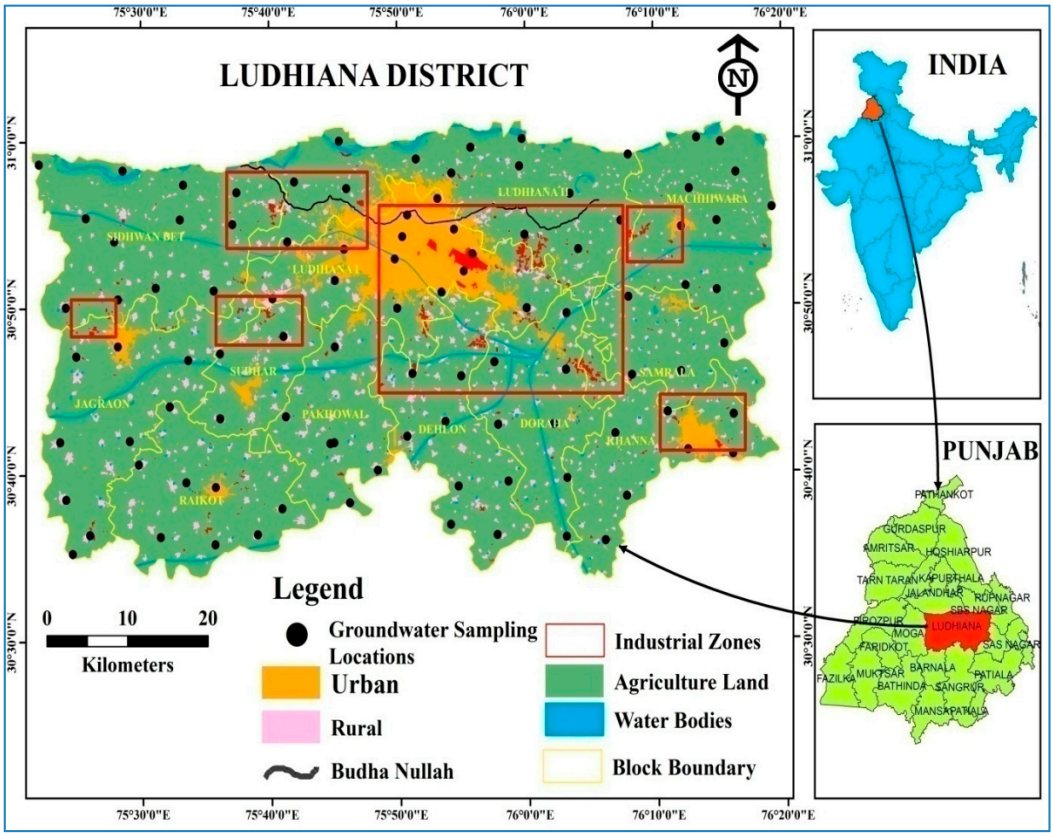

Figure 1. The study area.

2.2. Hydrogeology

The study area consists of Indo-Gangetic alluvium of quaternary age. Subsurface strata consist of clay, fine sand, medium sand, and hard clay. Moreover, kankar and gravel with sand are also present in some places. Two aquifers, confined and unconfined, mainly exist in the area and the subsurface water flows from N–SW and E–SW. The lithological data of the study area indicate the presence of many sand beds forming the principal aquifers separated by clay beds at various depths. It consists of five prominent sand horizons down to 400 m depth separated by thick clay horizons. The first aquifer generally occurs between 10 and 30 m. The second through fifth occur between 50 and 120 m, 150 and 175 m, 200 and 250 m, and 300 and 400 m, respectively. The depth to water level in the area ranges between 9 and 26 m below ground level (bgl). During the premonsoon period, the depth to water level varies between 4 and 31 m bgl, and postmonsoon, it ranges between 3 and 27 m bgl [33].

2.3. Collection of Samples and Analysis

Ninety-nine groundwater sampling locations (93 deep tube wells with depths ranging from 90 to 150 m and 6 shallow tube wells from 10 to 20 m deep), as shown in Figure 1, were sampled to cover the entire study area. Samples were collected during premonsoon (April–May) and postmonsoon (November–December) periods of 2018. The premonsoon and postmonsoon periods were defined as 1–2 months before and after the monsoon, respectively. The schedule of the sample collection is given in Supplementary Table S1. The coordinates of all the sampling locations were determined with a portable global positioning system (GARMIN Etrex 10). Standard protocols as prescribed in standard methods were followed during sampling and preserving the samples [34]. Glass bottles of 1000 mL capacity were utilized for sample collection. Sample bottles were washed by 1:1 HNO_3 and rinsed three times using triple-distilled water. Further, bottles were dried in a hot air oven at a temperature of 80 °C for 4 h. Cellulose filter paper (Whatman® filter paper, grade 42, GE Healthcare Companies, UK)

was used to filter groundwater samples. For the preservation of groundwater samples, each sample was acidified by adding 2 mL of HNO_3 to pH < 2, and acidified samples were put into an ice box. Each sample was labeled properly to prevent misidentification between samples and it was ensured that no air bubbles were present in the samples. Within 12 h of sampling, all water samples were transferred to the laboratory and stored at 4 °C for further analysis.

Analysis of ESEs, namely, As, Al, Cr, Hg, Fe, Ni, Se, and Pb, was accomplished with an atomic absorption spectrophotometer (model AAS 4141, Electronics Corporation of India Ltd., Hyderabad, India). Hollow cathode lamps were used for determining the As, Al, Cr, Hg, Fe, Ni, Se, and Pb at different wavelengths of 193.7, 309.3, 357.9, 253.7, 248.3, 232.0, 196.0, and 217.0 nm, respectively. Cr, Fe, Ni, and Pb were determined by the aspirating direct air–acetylene flame method with lamp currents of 7, 5, 3.5, and 10 mA, respectively. Al and Hg were estimated by the aspirating direct nitrous-oxide–acetylene flame method with a lamp current of 10 mA and the cold vapor atomic absorption spectrophotometer method with a lamp current of 5 mA, respectively. As and Se were determined by the continuous hydride generation method using nitrogen–acetylene gases with a lamp current of 10 mA.

2.4. Reagents, Standards, and Quality Assurance

High-purity, analytical-grade reagents and chemicals were used during the entire process for analyzing the heavy metals in groundwater samples. All the reagents and standards were prepared with triple-distilled water throughout the experimental work. For quality analysis, ready-made standard stock solutions of selected heavy metals of the concentration 1000 mg/L in HNO_3 were used (CDH Pvt. Ltd., New Delhi, India). To prepare calibration curves of each metal, four standard solutions for each metal at different concentrations were prepared. AAS was aspirated with blanks (triple-distilled water) and by zeroing the instrument at regular intervals to ensure its accuracy. Also, after analysis of 10 groundwater samples, 1 sample was examined in triplicate, so that consistent outcomes were maintained. The standard error between standards and measured samples were <5% [18,23].

2.5. Statistics and GIS Analysis

For statistical analysis, IBM Statistical Package for Social Sciences (SPSS®, version 25, IBM, New York, NY, USA) was used. The basic descriptive statistics feature of the package was used to analyze the range, mean, standard deviation, and so forth. For the paired *t*-test, the normality of the period differences was checked using the Kolmogorov–Smirnov test, and the compare mean module of SPSS was used to calculate the *p*-value. Pearson's correlation was performed with the assistance of the correlate module/bivariate correlations modules in SPSS. The Ludhiana district base map was digitized using ArcGIS® (version 10.4), ESRI, India. All the spatial and attribute data were input in the database of ArcGIS. All the thematic maps were prepared using the spatial analysis tools and the inverse distance weighted (IDW) interpolation technique. In this study, the search radius of 12 points was selected. The IDW interpolation technique uses the measured values of the surrounding locations to interpolate the values the prediction location.

2.6. Evaluation of Groundwater Quality by Indexing Approach

In this study, two pollution indexing approaches were applied to determine the groundwater quality and they are explained in the following subsections.

2.6.1. HPI

The HPI method was used to calculate the overall heavy metal contamination in groundwater. This method primarily depends on two factors: unit weightage (W_i) and the standard prescribed limit

(S_i) of each heavy metal. HPI calculation is based on the weighted arithmetic mean and, in this study, the HPI model, as developed and reported by Mohan et al. [35], described in Equation (1), was applied:

$$\text{HPI} = \frac{\sum_{i=1}^{n} W_i Q_i}{\sum_{i=1}^{n} W_i} \quad (1)$$

where W_i and Q_i are the unit weight and subindex of the *i*th parameter, respectively, and n is the number of parameters/ESEs considered. Unit weightage W_i is inversely proportional to the S_i, the recommended standard permissible limit of *i*th parameter in milligrams per liter, of all the selected heavy metals and was calculated by using Equation (2):

$$W_i \propto \frac{1}{S_i} \longrightarrow W_i = \frac{K}{S_i} \quad (2)$$

where K is the constant of proportionality, the value of which ranges from 0 to 1.The subindex (Q_i) for each heavy metal in Equation (1) was calculated by using Equation (3):

$$Q_i = \sum_{i=1}^{n} \frac{(M_i(-)\, I_i)}{(S_i - I_i)} \times 100 \quad (3)$$

where M_i and I_i are the analytical concentration and ideal value of the *i*th parameter/heavy metal in milligrams per liter, respectively. S_i is the recommended standard permissible limit of the *i*th parameter in milligrams per liter. In Equation (3), the (-) sign indicates the numerical difference between two values, eliminating the algebraic sign. The critical value of the HPI is 100, greater than which ingestion of groundwater will pose serious health effects to the human body [36]. The HPI method has previously been used to evaluate the status of metal pollution in surface water bodies, such as the River Bogayi in Turkey [37] and the Harike Wetland in Punjab, India [38]. The HPI in groundwater studies has also been used in Iran [39], Bangalore [40], Jharkhand [41], and West Bengal [42].

2.6.2. MI

The MI demonstrates the overall groundwater quality with respect to the heavy metal pollution. It was calculated using Equation (4), as defined by Tamasi and Cini [43]:

$$\text{MI} = \sum_{i=1}^{n} \frac{C_i}{(MAC)_i} \quad (4)$$

where C_i is the monitored concentration of the *i*th heavy metal (mg/L) and $(MAC)_i$ is the maximum allowable concentration of the *i*th metal. The threshold value for the MI quality index is 1. MI > 1 indicates water quality may not be suitable for long-term use due tothe potential for harmful chronic exposure.

2.7. Human Health Risk Assessment

The metal-contaminated groundwater could pose critical health risks via two common routes: ingestion (through drinking) and dermal exposure (through skin absorption). The United States Environmental Protection Agency (US EPA) has proposed a model for human health risk. The intake dose of ingestion and dermal activities was calculated using Equations (5) and (6), as suggested by the US EPA [44]:

$$\text{Intake}_{\text{ingestion}} = \frac{C \times \text{IR}_{\text{ingestion}} \times \text{EF} \times \text{ED}}{\text{BW} \times \text{AT}} \quad (5)$$

$$\text{Intake}_{\text{dermal}} = \frac{C \times K_p \times \text{ET} \times \text{CF} \times \text{EF} \times \text{ED} \times \text{EV}}{\text{BW} \times \text{AT}}. \quad (6)$$

A description of the parameters used in the above equations for adults and children is given in Supplementary Table S2.

2.7.1. Noncarcinogenic Risk Assessment

The noncarcinogenic health risk of each metal was assessed by calculating the hazard quotient (HQ). The HQ was calculated by dividing the intake value by the reference dose (RfD) using Equations (7) and (8). $RfD_{ingestion}$ represents the reference dose for ingestion of a selected metal, which was obtained from US EPA IRIS [45] and Li et al. [46], and RfD_{dermal} is the dermal reference dose calculated according to Equation (9) using the gastrointestinal absorption factor (GIABS) of selected metals, as suggested by the US EPA [47].

Further, the hazard index (HI) was calculated to determine the total noncarcinogenic effect of metals in groundwater by adding the $HQ_{ingestion}$ and HQ_{dermal} intake pathways of all selected metals using Equation (10) and then calculating HI_{total} using Equation (11), as detailed by the US EPA [44]:

$$HQ_{ingestion} = \frac{Intake_{ingestion}}{RfD_{ingestion}} \quad (7)$$

$$HQ_{dermal} = \frac{Intake_{dermal}}{RfD_{dermal}} \quad (8)$$

$$RfD_{dermal} = RfD_{Ingestion} \times GIABS \quad (9)$$

$$HI_{ingestion} = \sum HQ_{ingestion};\ HI_{dermal} = \sum HQ_{dermal} \quad (10)$$

$$HI_{total} = HI_{ingestion} + HI_{dermal}. \quad (11)$$

All the $RfD_{ingestion}$ and RfD_{dermal} values are presented in Supplementary Tables S3 and S4, respectively. Groundwater samples having $HI_{total} > 1$ suggest detrimental noncarcinogenic health effects to humans, whereas $HI_{total} < 1$ suggests that the groundwater would not pose any impact on human health [48].

2.7.2. Carcinogenic Risk Assessment

Exposure to polluted groundwater might create cancer-causing effects to humans. In this study, As, Cr, and Pb were considered as carcinogenic substances and the total carcinogenic risk (R_{total}) was calculated using Equations (12)–(15) [49]. As there was no specified cancer slope factor (CSF) for metals such as Al, Fe, Hg, Ni, and Se, carcinogenic risk was not calculated for these metals.

$$R_{ingestion} = Intake_{ingestion} \times CSF_{ingestion} \quad (12)$$

$$R_{dermal} = Intake_{dermal} \times CSF_{dermal} \quad (13)$$

$$R_{ingestion} = \sum R_{ingestion};\ R_{dermal} = \sum R_{dermal} \quad (14)$$

$$R_{Total} = R_{ingestion} + R_{dermal}. \quad (15)$$

If the R_{total} value is less than 1×10^{-6}, the chances of cancer risk are considered to be negligible, while an R_{total} value more than 1×10^{-4} indicates a substantial cancer risk [45]. CSF values of ingestion and dermal exposure were obtained from the Li et al. [46] and US EPA [47] (Supplementary Table S3).

3. Results and Discussion

3.1. Environmentally Sensitive Elements in Groundwater

Table 1 depicts the level of contamination of the groundwater samples with various ESEs, during premonsoon and postmonsoon periods, in comparison to the Bureau of Indian Standards (BIS) [50]. Further, the geospatial variation of ESEsin the groundwater of the study area is shown in Figure 2. The IDW interpolation technique of ArcGIS software (version 10.4), was used to prepare the spatial distribution maps.

Table 1. Environmentally sensitive elements (ESEs) in groundwater during pre- and postmonsoon periods.

ESEs (mg/L)	# BIS10500: 2012 Limit (mg/L)	Premonsoon			Postmonsoon		
		Range	Mean ± SD	No. of Samples above Limit	Range	Mean ± SD	No. of Samples above Limit
Al	0.2 *; 0.03 **	ND–0.847	0.255 ± 0.172	57 *;94 **	0.014–1.186	0.346 ± 0.262	62 *;94 **
As_{total}	0.05 *; 0.01 **	ND–0.021	0.0036 ± 0.004	0 *; 15 *	ND–0.020	0.0044 ± 0.0051	0 *;14 **
Cr_{total}	0.05 *	ND–0.078	0.021 ± 0.018	6 *	ND–0.158	0.033 ± 0.031	25 *
Fe	0.3 *	0.004–0.942	0.281 ± 0.143	38 *	0.120–1.010	0.321 ± 0.151	45 *
Hg	0.001 *	ND–0.004	0.0007 ± 0.0005	2 *	ND–0.005	0.00013 ± 0.0007	3 *
Ni	0.02 *	ND–0.786	0.155 ± 0.171	72 *	ND–1.272	0.204 ± 0.226	79 *
Pb	0.010 *	ND–0.435	0.070 ± 0.072	88 *	ND–0.656	0.098 ± 0.106	91 *
Se	0.010 *	ND–0.052	0.011 ± 0.010	31 *	ND–0.040	0.010 ± 0.008	39 *

Note: * (Permissible Limit); ** (Acceptable Limit); ND—Not Detected; # Bureau of Indian Standards (BIS 10500: 2012).

It can be seen from Table 1 that in the case of Pb contamination, 88 and 91 samples exceeded the permissible limits during premonsoon and postmonsoon periods, respectively. The concentration of Pb in the NE-SE parts of the study area was found to be higher during both periods. In addition, the concentration of Ni exceeded the permissible limit in 72 samples during the premonsoon period and in 79 samples during the postmonsoon period. The concentration of Al also exceeded the permissible limit in 57 and 62 samples during the pre- and postmonsoon periods, respectively. Shrivastava [26] also reported high concentrations of Al, Ni, and Pb in groundwater samples collected from other districts of Punjab, which are located in the vicinity of the study area. The mean concentration of the ESEs was observed to increase during the postmonsoon period. The paired *t*-test for pre- and postmonsoon periods showed significant variation during the postmonsoon period, as there was a p-value < 0.05 for seven parameters, namely, Fe, Pb, Ni, Al, Se, Cr, and As. However, Hg did not show a significant variation. The probable reason could be the lesser/statistically insignificant number of samples (two premonsoon and three postmonsoon samples) indicating Hg contamination. Paired *t*-tests for pre- and postmonsoon periods for all heavy metals are shown in the Supplementary Table S5. The reasons for the increased concentration postmonsoon could be due to dissolution of the metals from parent bedrock into groundwater at higher temperatures during the monsoon season [18]. In general, concentrations of most of the ESEs were found to be high in samples collected in and around industrial areas. Therefore, it could also be attributed to the seepage of ESEs from the surface to the aquifer during monsoon season in the industrial areas. Similar studies from other parts of India have also reported that groundwater beneath industrial establishments is generally contaminated with heavy metals [51–53]. Although Fe is an essential element for human beings, a higher Fe concentration in drinking water can cause certain health impacts [54]. In 38 and 45 samples, the Fe concentration was above the permissible limit during premonsoon and postmonsoon periods, respectively. For Cr_{total}, only 6 samples were above the permissible limit during the premonsoon period, while in the postmonsoon period, the concentration of Cr_{total} in groundwater samples exceeded the limit in 25 samples. Brindha and Elango also reported the higher concentration of Cr near the industrial sites of Chennai, India [55]. The concentration of As exceeded the acceptable limits in 10 and 15 groundwater samples collected during pre- and postmonsoon periods, respectively. Hg was found to be above the permissible limits in two and three samples from shallow wells located in and around the industrial area during pre- and postmonsoon periods, respectively. Higher concentrations of Hg and As in groundwater samples

around the industrialized region of Maharashtra, India were reported by Bhagure and Mirgane [56]. Further, mean concentrations of the various ESEs in groundwater samples were observed to be in the following order: Premonsoon—Fe > Al > Ni > Pb > Cr > Se > As > Hg; Postmonsoon—Al > Fe > Ni > Pb > Cr > Se > As > Hg.

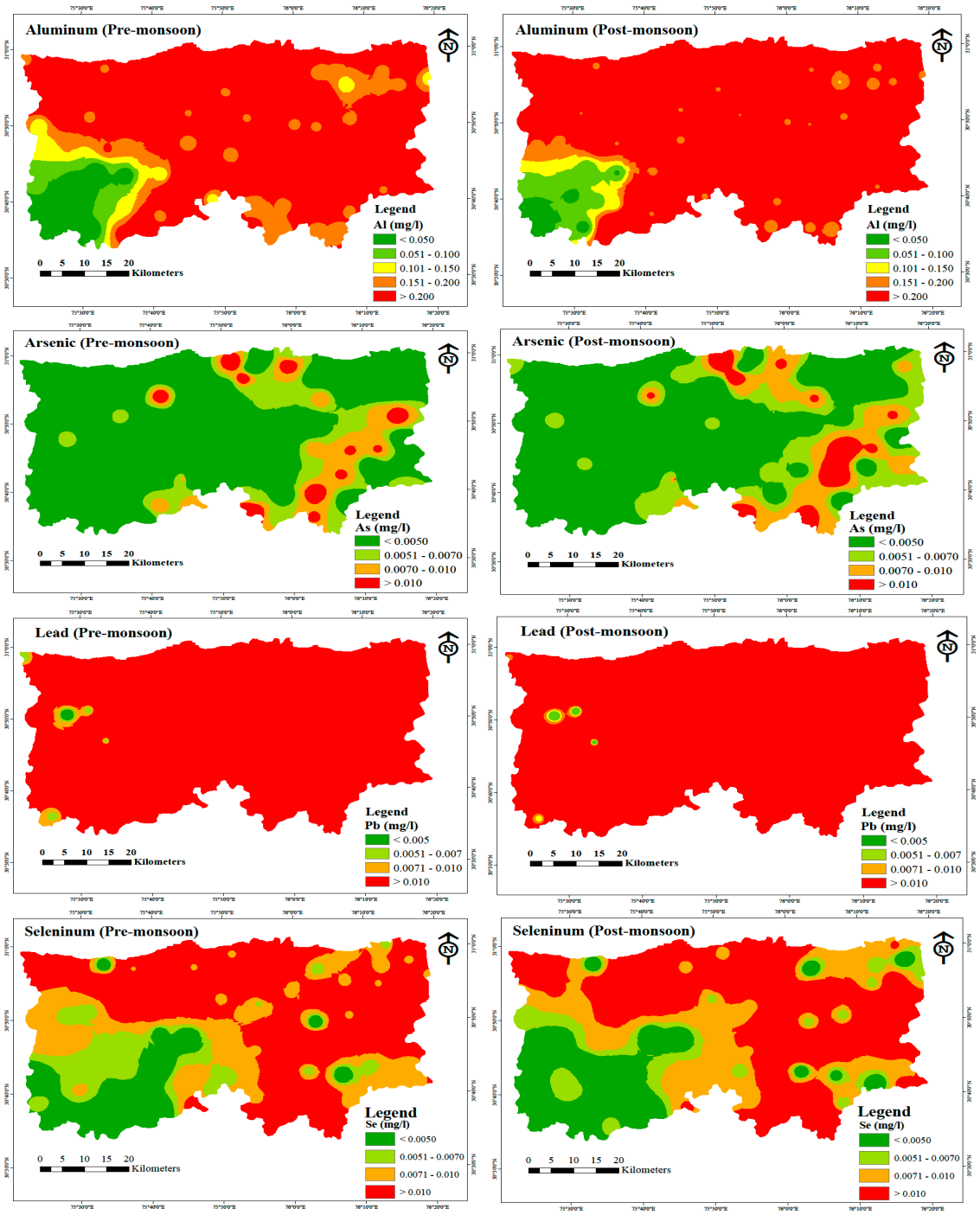

Figure 2. *Cont.*

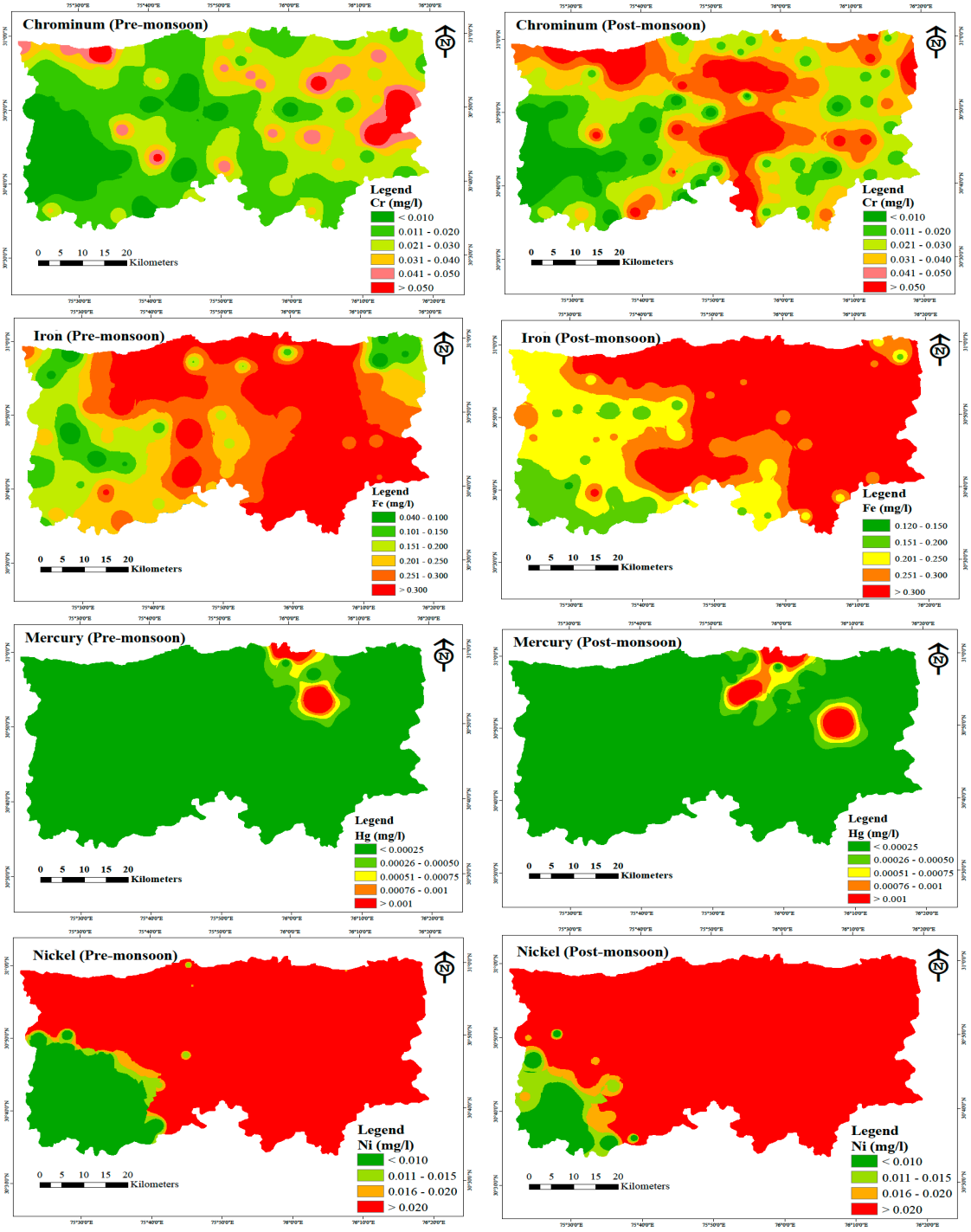

Figure 2. Geospatial variation of ESEs during pre- and postmonsoon periods.

3.2. *Pearson's Inter-ESE Correlation*

The interrelationship between the ESEs was evaluated using Pearson's correlation. The correlations of heavy metals (As, Al, Cr, Hg, Fe, Ni, Se, and Pb) during pre- and postmonsoon periods are presented in Tables 2 and 3, respectively. The critical values for Pearson's coefficient (r) for 99 groundwater samples were 0.197 and 0.257 at $p \leq 0.05$ and $p \leq 0.01$, respectively. Correlation analysis at the $p = 0.01$ and 0.05 levels indicated significant relationships between the metals Al–Se, As–Ni, Fe–Ni, Ni–Pb, Ni–Se, and Pb–Se and Al–Fe, As–Fe, As–Se, Cr–Ni, Cr–Pb, Fe–Pb, Fe–Se, Hg–Pb, respectively, during the premonsoon period. Also, during the postmonsoon period, the correlation results indicated a

positive relation between metals such as Al–Se, As–Se, Fe–Ni, Fe–Pb, Ni–Pb, Ni–Se, and Pb–Se at the 0.01 level and Cr–Hg, Cr–Se, and Fe–Se at the 0.05 level. Strong positive relations indicate that Pb, Ni, and Se have the same source of pollution during both periods, which is evident from the outcomes correlating higher concentrations of these metals in and around the industrial areas. It was implied that, due to the strong correlation between Fe and Ni (r = 0.362) and Ni and Pb (r = 0.417) during both periods, their source of contamination could be from dumping of electroplating industrial waste, which is very common in the study area [57].

Table 2. Pearson's correlation matrix during premonsoon period.

ESEs	Al	As	Cr	Fe	Hg	Ni	Pb	Se
Al	1	0.147	0.120	0.243 *	0.077	0.139	0.130	0.358 **
As		1	0.192	0.224 *	0.103	0.264 **	0.143	0.229 *
Cr			1	0.076	0.097	0.207 *	0.242 *	0.178
Fe				1	0.122	0.362 **	0.227 *	0.207 *
Hg					1	0.152	0.198 *	0.158
Ni						1	0.301 **	0.340 **
Pb							1	0.282 **
Se								1

Note: ** Correlation significant at the 0.01 level (two-tailed); * Correlation significant at the 0.05 level (two-tailed).

Table 3. Pearson's correlation matrix during postmonsoon period.

ESEs	Al	As	Cr	Fe	Hg	Ni	Pb	Se
Al	1	0.112	0.193	0.055	0.060	0.113	0.100	0.365 **
As		1	0.169	0.061	0.121	0.197	0.147	0.271 **
Cr			1	0.096	0.246 *	0.060	0.145	0.214 *
Fe				1	0.103	0.328 **	0.309 **	0.228 *
Hg					1	−0.066	0.005	0.163
Ni						1	0.417 **	0.374 **
Pb							1	0.282 **
Se								1

Note: ** Correlation significant at the 0.01 level (two-tailed); * Correlation significant at the 0.05 level (two-tailed).

3.3. HPI and MI

Table 4 presents the classification of groundwater in terms of the indices HPI and MI. The classification was adapted from Sankar (2019) [40]. The geospatial representation of water quality indices based on HPI and MI during the premonsoon and postmonsoon periods are shown in Figures 3 and 4, respectively. The HPI-based groundwater assessment revealed that 35.4% of the groundwater samples during the premonsoon period and 52.5% of the groundwater samples during the postmonsoon period were above the critical pollution index of 100. This indicates that at these sampling points, the groundwater may pose health risks to humans if used for drinking. It can also be seen from Figure 3 that the sampling wells near the industrial area and along the channel (BudhaNullah) which receives the industrial effluent show higher HPI values. On the other hand, the analysis using the MI indicated that 79.8% and 86.9% of the samples showed values greater than 1, which is the critical MI. Figure 4 depicts the spatial variation of the MI in the study area. The MI also exhibited a similar geographical pattern as that of the HPI in terms of level of heavy metal pollution. However, the variations in the geographical spread of each class of water quality seen in Table 4 and Figures 3 and 4 could be due to the difference in the definition of the indices. The HPI provides an aggregated influence of individual heavy metals on the total water quality, whereas the MI gives only an exceedance value from the standards. The quality of groundwater evaluated using both the HPI and the MI strongly suggests that exposure to this groundwater may cause detrimental effects to human health.

Table 4. Classification based on the heavy metal pollution index (HPI) and the metal index (MI).

		No. of Groundwater Samples			
Index	**Classification**	**Premonsoon**	**Postmonsoon**	**% Premonsoon**	**% Postmonsoon**
HPI	<25: Excellent	15	10	15.1%	10.1%
	26–50: Good	15	7	15.1%	7.1%
	51–75: Poor	16	21	16.2%	21.2%
	76–100: Very poor	18	9	18.2%	9.1%
	>100: Unsuitable for drinking	35	52	35.4%	52.5%
MI	<0.3: Very pure	5	2	5.1%	2%
	0.3–1: Pure	15	11	15.1%	11.1%
	1–2: Slightly affected	32	27	32.3%	27.2%
	2–4: Moderately affected	31	36	31.3%	36.4%
	4–6: Strongly affected	11	12	11.1%	12.1%
	>6: Seriously affected	5	11	5.1%	11.1%

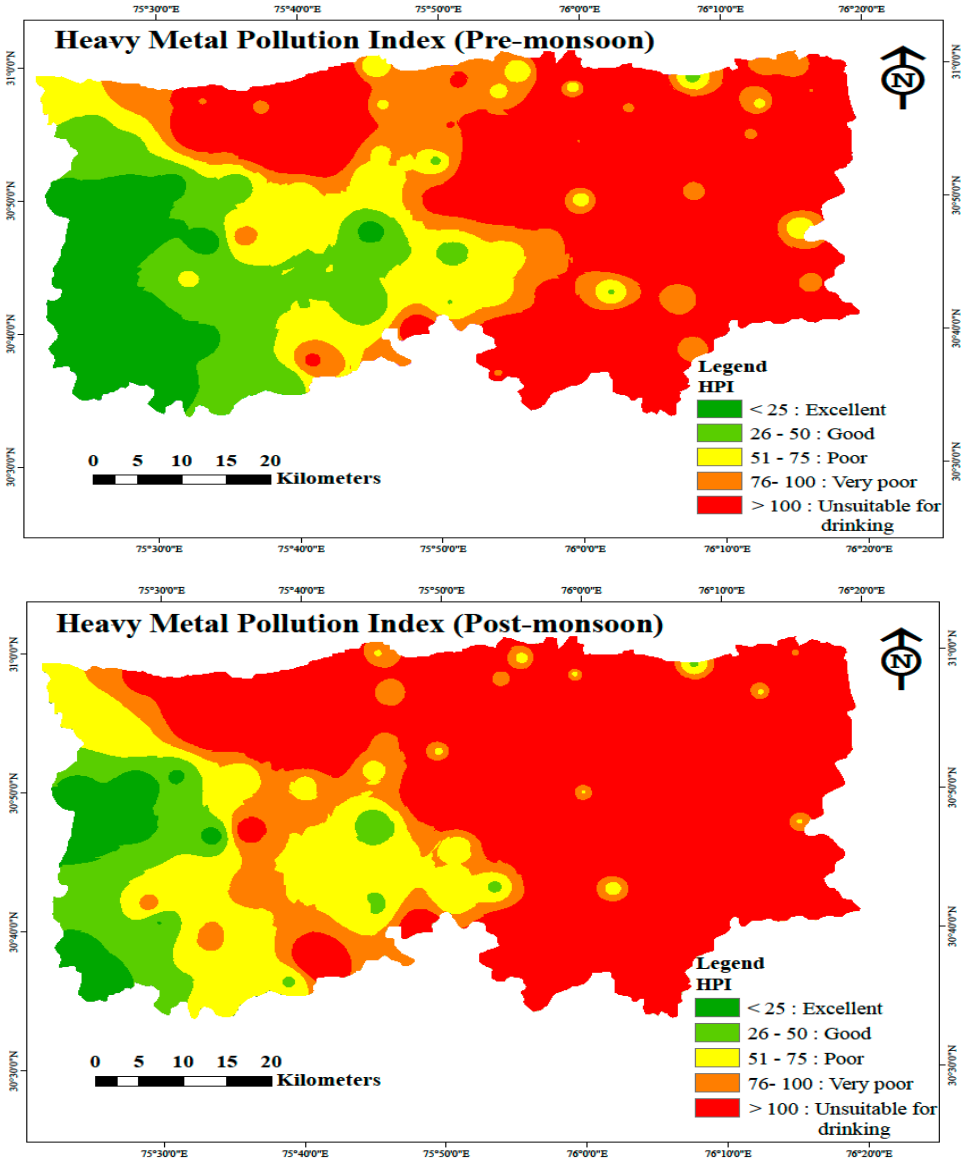

Figure 3. Geospatial variation of the HPI during pre- and postmonsoon periods.

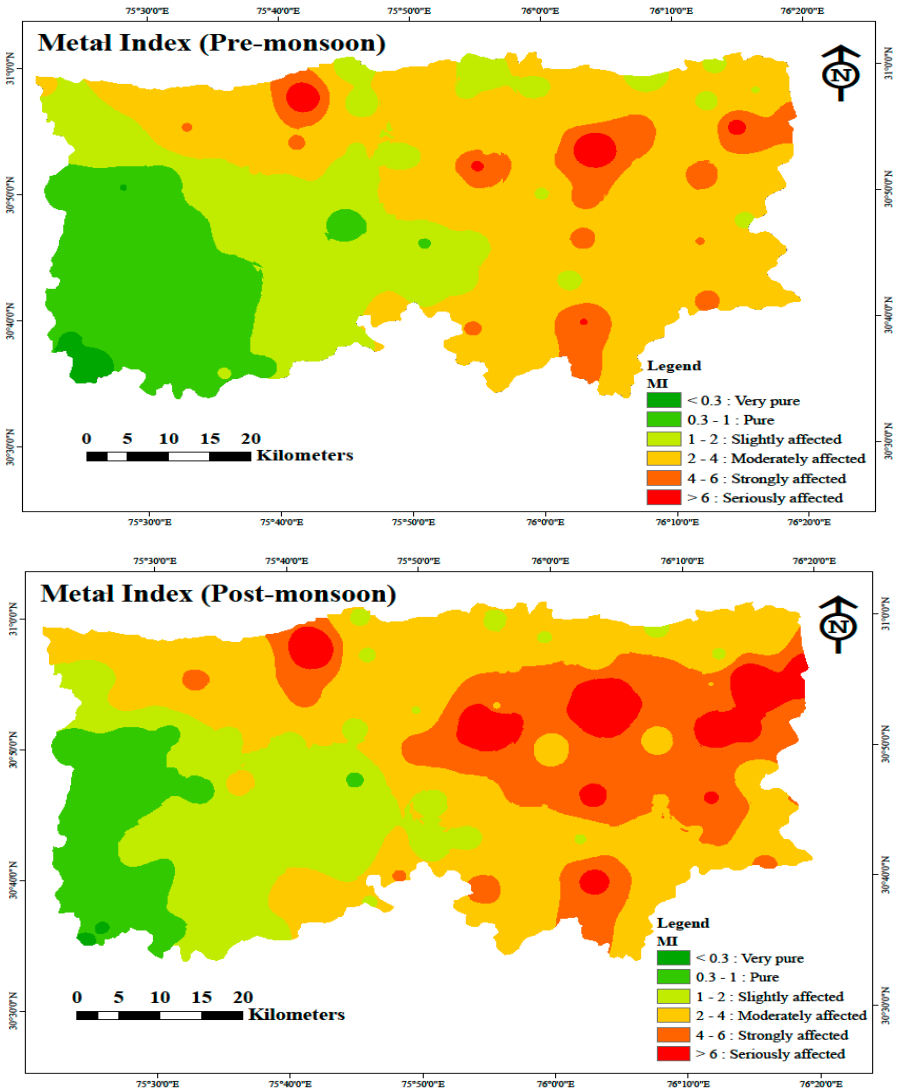

Figure 4. Geospatial variation of the MI during pre- and postmonsoon periods.

3.4. Health Risk Assessment

The concentration of ESEs in groundwater was examined to assess the health risk through ingestion and dermal pathways for adults and children, and the outcomes of this analysis are presented in Table 5.

Table 5 shows that the $HQ_{ingestion}$ and HQ_{dermal} during the premonsoon period followed the order of Pb > As > Ni > Cr > Se > Fe > Al > Hg and Cr > Ni > As > Hg > Se > Pb > Fe > Al, respectively, for both adults and children. However, during the postmonsoon period, the order of $HQ_{ingestion}$ and HQ_{dermal} was Pb > As > Cr > Ni > Se > Fe > Hg > Al and Cr > Ni > As > Hg > Pb > Se > Fe > Al, respectively, for both adults and children. Pb and Cr were found to be the main contributors to HQ. The HQ values for all heavy metals were found to be < 1 for both ingestion and dermal pathways during both seasons, except for Pb. Moreover, Pb was found to be > 1 for children through the ingestion pathway, and mean observed values were 1.32 and 1.87 during the pre- and postmonsoon periods, respectively (Table 5). It can be inferred that, in the study area, Pb contamination has a higher potential to pose noncarcinogenic health risks to children. Similar health risk assessment studies reported from China found higher health risks due to heavy metals in children than adults [58].

Table 5. Hazard quotient (HQ) of different ESEs during pre- and postmonsoon periods.

			Metals							
			Al	**As**	**Cr**	**Fe**	**Hg**	**Ni**	**Pb**	**Se**
Children [a]	$HQ_{ingestion}$	Range	$0–5.59 \times 10^{-2}$	0–4.62	0–1.72	$0–8.88 \times 10^{-2}$	$0–8.80 \times 10^{-1}$	0–2.59	0–8.20	$0–6.86 \times 10^{-2}$
		Mean	1.68×10^{-2}	7.91×10^{-1}	4.62×10^{-1}	2.65×10^{-2}	1.56×10^{-2}	5.13×10^{-1}	1.32	1.53×10^{-1}
	HQ_{dermal}	Range	$0–3.73 \times 10^{-4}$	$0–3.08 \times 10^{-2}$	$0–8.80 \times 10^{-1}$	$0–5.92 \times 10^{-4}$	$0–8.38 \times 10^{-2}$	$0–8.65 \times 10^{-2}$	$0–5.47 \times 10^{-3}$	$0–4.58 \times 10^{-3}$
		Mean	1.12×10^{-4}	5.27×10^{-3}	2.37×10^{-1}	1.77×10^{-4}	1.48×10^{-3}	1.71×10^{-2}	8.82×10^{-4}	1.02×10^{-3}
Adult [a]	$HQ_{ingestion}$	Range	$0–2.80 \times 10^{-2}$	0–2.31	$0–8.58 \times 10^{-1}$	$0–4.44 \times 10^{-2}$	$0–4.40 \times 10^{-1}$	0–1.30	0–4.10	$0–3.43 \times 10^{-1}$
		Mean	8.42×10^{-3}	3.96×10^{-1}	2.31×10^{-1}	1.32×10^{-2}	7.78×10^{-3}	2.57×10^{-1}	6.62×10^{-1}	7.64×10^{-2}
	HQ_{dermal}	Range	$0–1.47 \times 10^{-4}$	$0–1.22 \times 10^{-2}$	$0–3.48 \times 10^{-1}$	$0–2.34 \times 10^{-4}$	$0–3.31 \times 10^{-2}$	$0–3.42 \times 10^{-2}$	$0–2.16 \times 10^{-3}$	$0–1.81 \times 10^{-3}$
		Mean	4.44×10^{-5}	2.09×10^{-3}	9.38×10^{-2}	6.98×10^{-5}	5.86×10^{-4}	6.77×10^{-3}	3.49×10^{-4}	4.03×10^{-4}
Children [b]	$HQ_{ingestion}$	Range	$0–7.83 \times 10^{-2}$	0–4.40	0–3.48	$0–9.52 \times 10^{-2}$	0–1.10	0–4.20	$0–1.24 \times 10^{-1}$	$0–5.28 \times 10^{-1}$
		Mean	2.29×10^{-2}	9.73×10^{-1}	7.46×10^{-1}	3.03×10^{-2}	2.89×10^{-2}	6.74×10^{-1}	1.87	1.39×10^{-1}
	HQ_{dermal}	Range	$0–5.22 \times 10^{-4}$	$0–2.93 \times 10^{-2}$	0–1.78	$0–6.35 \times 10^{-4}$	$0–1.05 \times 10^{-1}$	$0–1.40 \times 10^{-1}$	$0–1.58 \times 10^{-2}$	$0–3.52 \times 10^{-3}$
		Mean	1.53×10^{-4}	6.49×10^{-3}	3.83×10^{-1}	2.02×10^{-4}	2.75×10^{-3}	2.28×10^{-2}	1.30×10^{-3}	9.26×10^{-4}
Adult [b]	$HQ_{ingestion}$	Range	$0–3.91 \times 10^{-2}$	0–2.20	0–1.74	$0–4.76 \times 10^{-2}$	$0–5.50 \times 10^{-1}$	0–2.10	0-6.19	$0–2.64 \times 10^{-1}$
		Mean	1.14×10^{-2}	4.87×10^{-1}	3.73×10^{-1}	1.52×10^{-2}	1.44×10^{-2}	3.37×10^{-1}	9.33×10^{-1}	6.95×10^{-2}
	HQ_{dermal}	Range	$0–2.06 \times 10^{-4}$	$0–1.16 \times 10^{-2}$	$0–7.05 \times 10^{-1}$	$0–2.51 \times 10^{-4}$	$0–5.80 \times 10^{-2}$	$0–5.53 \times 10^{-2}$	$0–3.26 \times 10^{-3}$	$0–1.39 \times 10^{-3}$
		Mean	6.03×10^{-5}	2.57×10^{-3}	1.51×10^{-1}	8.00×10^{-5}	1.26×10^{-3}	8.88×10^{-3}	5.14×10^{-4}	3.66×10^{-4}

Note: a—Premonsoon; b—Postmonsoon.

Further, the total hazard index (HI_{total}) was calculated for both children and adults during both periods and it was observed that HI_{total} mean values for adults and children were > 1 in the premonsoon (1.76 and 3.57, respectively) and postmonsoon (2.41 and 4.90, respectively) periods, as shown in Table 6. Figure 5 shows that during the premonsoon period, 76.5% and 93.5% of the study area had HI_{total} > 1 for adults and children, respectively, and during the postmonsoon period, 89.3% and 98.9% of the study area had HI_{total} > 1 for adults and children, respectively. It was also observed that HI_{total} values of children were higher than adults for ingestion and dermal pathways. This is because children weigh less than adults. A similar observation from Punjab was reported by Sharma et al. [18].

Table 6. HI_{total} and total carcinogenic health risk (R_{total}).

Total Health Risk	Category	Calculated Mean
HI_{total} (Premonsoon)	Children	3.57
	Adult	1.76
HI_{total} (Postmonsoon)	Children	4.90
	Adult	2.41
R_{total}(Premonsoon)	Children	8.87×10^{-4}
	Adult	4.43×10^{-4}
R_{total} (Postmonsoon)	Children	1.37×10^{-3}
	Adult	6.85×10^{-4}

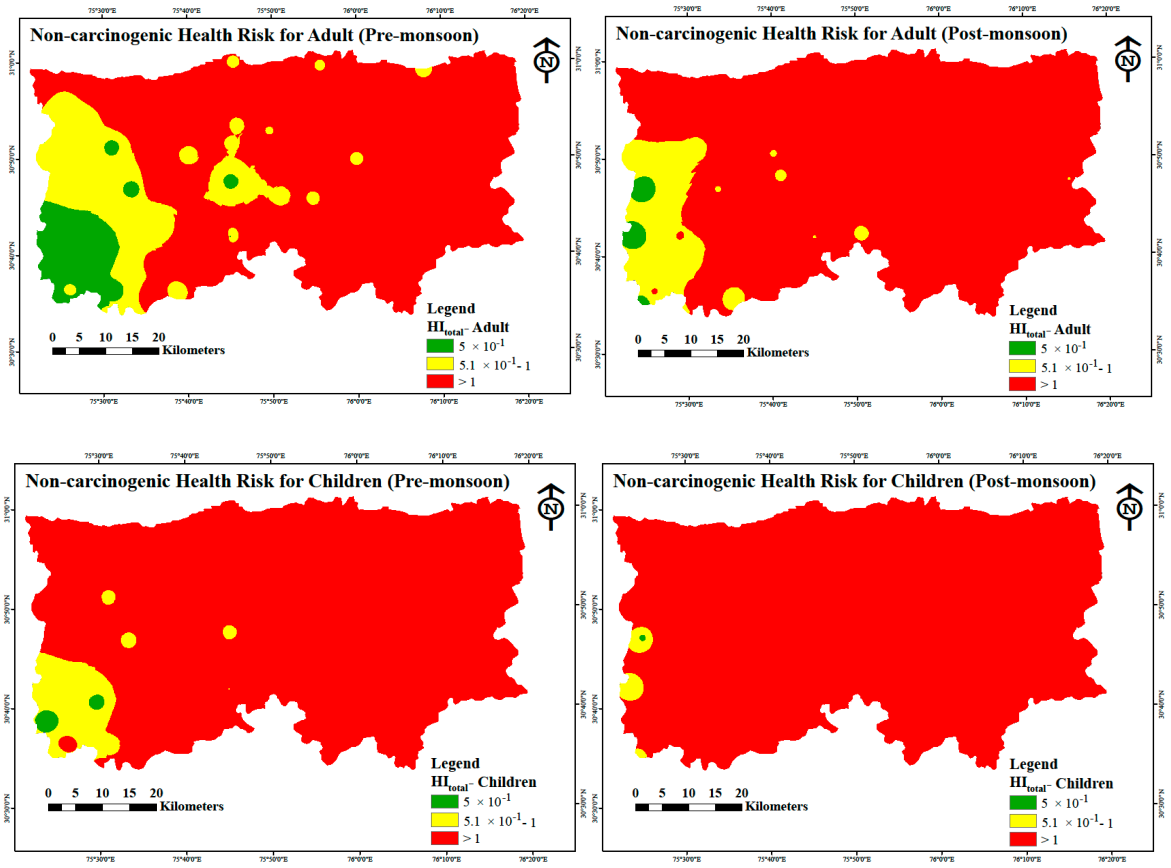

Figure 5. HI_{total} for adults and children during pre- and postmonsoon periods.

The total carcinogenic health risk (R_{total}) was also calculated through ingestion and dermal pathways during pre- and postmonsoon periods, as presented in Table 6, and its geospatial distribution

is presented in Figure 6. The calculated mean values for R_{total}, as shown in Table 6, are greater than 1×10^{-4}, which indicates potential carcinogenic effects.

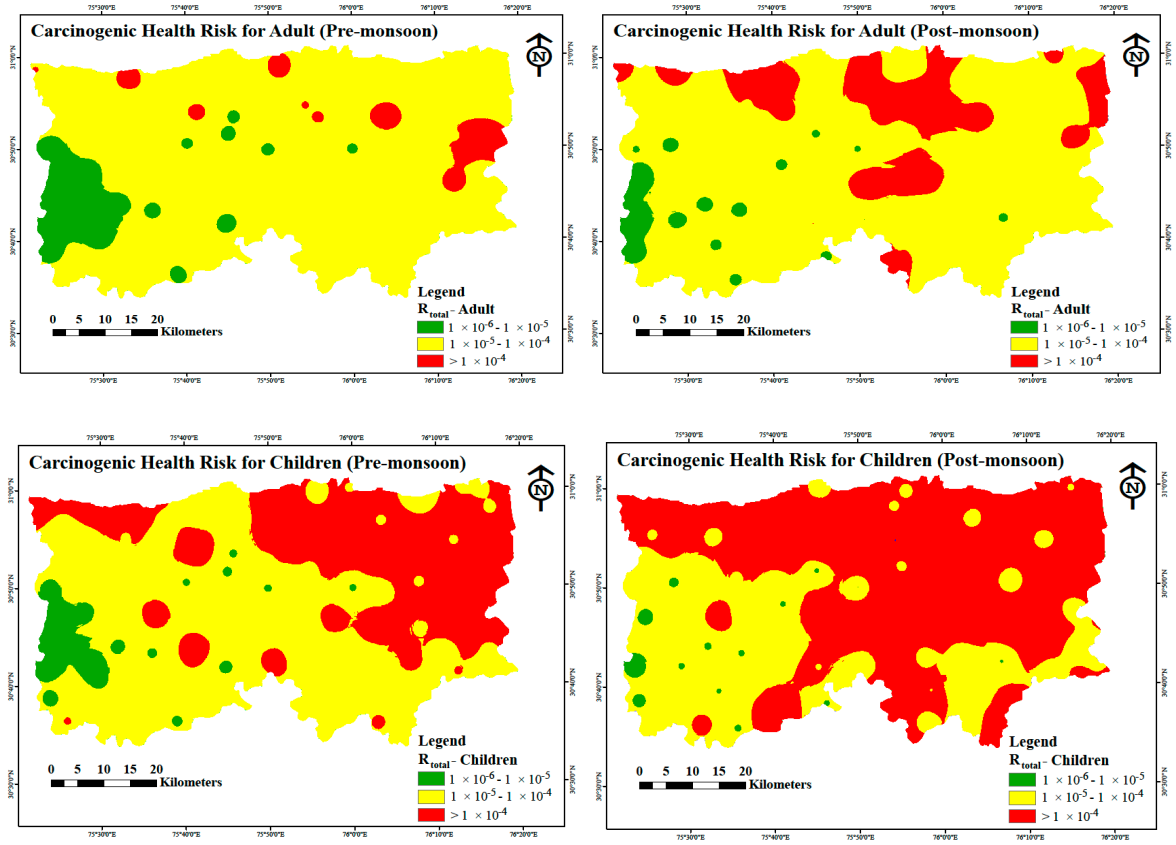

Figure 6. R_{total} for adults and children during pre- and postmonsoon periods.

4. Conclusions

Based on the findings of the study, it can be concluded that the groundwater of the study area can pose serious health impacts due to presence of ESEs. The spatial distribution of the ESEs in the groundwater and the Pearson's correlation of different metals clearly indicate the contribution of industrial activities to contaminating the groundwater. HPI-based water quality analysis revealed that 1734 and 2219 km^2 of the area were above the critical pollution index during pre- and postmonsoon periods, respectively. Further, MI-based analysis indicated that 3003 and 3328 km^2 of the area were above the threshold limit during the pre- and postmonsoon periods, respectively. The presence of ESEs in the groundwater of the study area can pose noncarcinogenic health risks. The carcinogenic health risks through ingestion and dermal pathways are mainly due to the presence of As, Pb, and Cr contamination. R_{total} for adults revealed that 167 and 635 km^2 of the study area posed carcinogenic health risks during pre- and postmonsoon periods, respectively. R_{total} for children showed that 1316 and 2314 km^2 of the study area could pose carcinogenic health risks during pre- and postmonsoon periods, respectively. The outcomes of this study will be helpful to understand the extent of ESE contamination in the groundwater of the study area and its effect on consumers due to long-term exposure. Therefore, it is recommended that ESEs should also be included in the routine monitoring of the groundwater, and evidence-based policies should be framed to mitigate ESE contamination of the groundwater in the region.

Supplementary Materials: The following are available online at http://www.mdpi.com/2073-4441/11/11/2350/s1, Tables S1–S5 present the supplementary data used in the analyses. Table S1: Schedule of sampling during premonsoon and post monsoon, Table S2: Description of exposure parameters for calculation of health risk assessment, Table S3: Reference dose ingestion value for heavy metals, Table S4: Reference dose dermal, skin permeability constant and cancer slope factor value for heavy metals, Table S5: Paired sample t – test for heavy metals during pre- and postmonsoon periods.

Author Contributions: D.D.S. planned the research methodology after extensive discussions with M.S. and S.J. D.D.S. also collected the samples and performed the analysis. Further, the findings of the analysis were statistically interpreted and presented in the form of a scientific manuscript after considerable input from P.S.T., M.S., and S.J. S.S. assisted in the generation of geospatial maps using ArcGIS.

Funding: No external funding and the APC was funded by first author D.D.S. from his personal funds.

Acknowledgments: The first author acknowledges the I.K. Gujral Punjab Technical University, Kapurthala, Punjab, India for providing him the opportunity to conduct his doctoral research in the area. He also gratefully acknowledges T.S. Sidhu, Director, Shaheed Bhagat Singh State Technical Campus, Ferozepur, and Brijendra Pateriya, Director, Punjab Remote Sensing Centre, Ludhiana, Punjab, India for providing support and laboratory facilities for this research work. The authors would like to thank the reviewers and editor for their constructive comments that helped in improving the manuscript.

Conflicts of Interest: The authors declare no conflicts of interest.

References

1. Bhutiani, R.; Kulkarni, D.B.; Khanna, D.R.; Gautam, A. Water quality, pollution source apportionment and health risk assessment of heavy metals in groundwater of an industrial area in North India. *Expo. Health* **2016**, *8*, 3–18. [CrossRef]
2. Prasanth, S.S.V.; Magesh, N.S.; Jitheshlal, K.V.; Chandrasekar, N.; Gangadhar, K. Evaluation of groundwater quality and its suitability for drinking and agricultural use in the coastal stretch of Alappuzha District, Kerala, India. *Appl. Water Sci.* **2012**, *2*, 165–175. [CrossRef]
3. Upadhyaya, D.; Survaiya, M.D.; Basha, S.; Mandal, S.K.; Thorat, R.B.; Haldar, S.; Goel, S.; Dave, H.; Baxi, K.; Trivedi, R.H.; et al. Occurrence and distribution of selected heavy metals and boron in groundwater of the Gulf of Khambhat region, Gujarat, India. *Environ. Sci. Pollut. Res.* **2014**, *21*, 3880–3890. [CrossRef] [PubMed]
4. Martinez-Lopez, S.; Martinez-Sanchez, M.J.; Gomez-Marinez, M.C.; Perez-Sirvent, C. Assessment of the risk associated with mining-derived inputs in a lagoon system. *Environ. Geochem. Health* **2019**, 1–12. [CrossRef] [PubMed]
5. Thakur, T.; Rishi, M.S.; Naik, P.K.; Sharma, P. Elucidating hydrochemical properties of groundwater for drinking and agriculture in parts of Punjab, India. *Environ. Earth Sci.* **2016**, *75*, 467–481. [CrossRef]
6. Rahman, M.M.; Islam, M.A.; Doza, M.B.; Muhib, M.I.; Zahid, A.; Mashura, S.M.; Tareq, S.M.; Kurasaki, M. Spatio-temporal assessment of groundwater quality and human health risk:A case study in Gopalganj, Bangladesh. *Expo. Health* **2017**, *10*, 167–188. [CrossRef]
7. Cao, S.; Duan, X.; Zhao, X.; Chen, Y.; Beibei, W.B.; Sun, C.; Zheng, B.; Weid, F. Health risks of children's cumulative and aggregative exposure to metals and metalloids in a typical urban environment in China. *Chemosphere* **2016**, *147*, 404–411. [CrossRef] [PubMed]
8. Elumalai, V.; Brindha, K.; Lakshmanan, E. Human exposure risk assessment due to heavy metalsin groundwater by pollution index and multivariate statistical methods: A case study from South Africa. *Water* **2017**, *9*, 234. [CrossRef]
9. Saleh, H.N.; Panahande, M.; Yousefi, M.; Asghari, F.B.; Oliveri, C.G.; Talaee, E.; Mohammadi, A.A. Carcinogenic and non-carcinogenic risk assessment of heavy metals in groundwater wells in Neyshabur Plain, Iran. *Biol. Trace Ele. Res.* **2018**, *190*, 251–261. [CrossRef] [PubMed]
10. Tiwari, A.K.; De Maio, M.; Amanzio, G. Evaluation of metal contamination in the groundwater of the Aosta Valley region, Italy. *Int. J. Environ. Res.* **2017**, *11*, 291–300. [CrossRef]
11. Venkatramanan, S.; Chung, S.Y.; Kim, T.H.; Prasanna, M.V.; Hamm, S.Y. Assessment and distribution of metals contamination in groundwater: a case study of Busan city, Korea. *Water Qual. Expo. Health* **2015**, *7*, 219–225. [CrossRef]
12. Khan, S.; Rauf, R.; Muhammad, S.; Qasim, M.; Din, I. Arsenic and heavy metals health risk assessment through drinking water consumption in the Peshawar district, Pakistan. *Human Eco. Risk Assess: An Inter. J.* **2015**, *22*, 581–596. [CrossRef]

13. Wongsasuluk, P.; Chotpantarat, S.; Siriwong, W.; Robson, M. Heavy metal contamination and human health risk assessment in drinking water from shallow groundwater wells in an agricultural area in UbonRatchathani province, Thailand. *Environ. Geochem. Health* **2014**, *36*, 169–182. [CrossRef] [PubMed]
14. Singh, A.; Saha, D.; Tyagi, A.C. Emerging issues in water resources management: Challenges and prospects. In *Water Governance: Challenges and Prospects*; Springer: Singapore, 2019; pp. 1–21. [CrossRef]
15. Purushotham, D.; Linga, D.; Netramani, S.; Sibasish, M.; Naga, V.G.; Venkatesham, K.; Saikrishna, K. Groundwater contamination in parts of Nalgonda district, Telangana, India as revealed by trace elemental studies. *J. Geol. Soc. India* **2017**, *90*, 447–458. [CrossRef]
16. Ravindra, K.; Mor, S. Distribution and health risk assessment of arsenic and selected heavy metals in groundwater of Chandigarh, India. *Environ. Pollut.* **2019**, *250*, 820–830. [CrossRef] [PubMed]
17. Singh, G.; Kamal, R.K. Heavy metal contamination and its indexing approach for groundwater of Goa mining region, India. *Appl. Water Sci.* **2017**, *7*, 1479–1485. [CrossRef]
18. Sharma, S.; Nagpal, A.K.; Kaur, I. Appraisal of heavy metal contents in groundwater and associated health hazards posed to human population of Ropar wetland, Punjab, India and its environs. *Chemosphere* **2019**, *227*, 179–190. [CrossRef] [PubMed]
19. Duggal, V.; Rani, A.; Mehra, R.; Balaram, V. Risk assessment of metals from groundwater in northeast Rajasthan. *J. Geol. Soc. India* **2017**, *90*, 77–84. [CrossRef]
20. Selvam, S.; Venkatramanan, S.; Sivasubramanian, P.S.Y.; Chung, S.Y.; Singaraja, C. Geochemical characteristics and evaluation of minor and trace elements pollution in groundwater of Tuticorin city, Tamil Nadu, India using geospatial techniques. *J. Geol. Soc. India* **2017**, *90*, 62–68. [CrossRef]
21. Lapworth, D.J.; Das, P.; Shaw, A.; Mukherjee, A.; Civil, W.; Petersen, J.O.; Gooddy, D.C.; Wakefield, O.; Finlayson, A.; Krishan, G.; et al. Deep urban groundwater vulnerability in India revealed through the use of emerging organic contaminants and residence time tracers. *Environ. Pollut.* **2018**, *240*, 938–949. [CrossRef] [PubMed]
22. Ahada, C.P.S.; Suthar, S. Groundwater nitrate contamination and associated human health risk assessment in southern districts of Punjab, India. *Environ. Sci. Pollut. Res.* **2018**, *25*, 25336–25347. [CrossRef] [PubMed]
23. Chabukdhara, M.; Gupta, S.K.; Kotecha, Y.; Nema, A.K. Groundwater quality in Ghaziabad district, Uttar Pradesh, India: Multivariate and health risk assessment. *Chemosphere* **2017**, *179*, 167–178. [CrossRef] [PubMed]
24. Kashyap, R.; Verma, K.S.; Uniyal, S.K.; Bhardwaj, S.K. Geospatial distribution of metal(loid)s and human health risk assessment due to intake of contaminated groundwater around an industrial hub of Northern India. *Environ. Monit. Assess.* **2018**, *190*, 136–153. [CrossRef] [PubMed]
25. Duggal, V.; Rani, A. Carcinogenic and non-carcinogenic risk assessment of metals in groundwater via ingestion and dermal absorption pathways for children and adults in Malwa region of Punjab. *J. Geol. Soc. India* **2018**, *92*, 187–194. [CrossRef]
26. Shirvastva, B.K. Elevated uranium and toxic elements concentration in groundwater in Punjab State of India: Extent of the problem and risk due to consumption of unsafe drinking water. *Water Qual. Expo. Health* **2014**, *7*, 407–421. [CrossRef]
27. World Health Organization (WHO). *Guidelines for Drinking Water Quality*, 4th ed.; WHO: Geneva, Switzerland, 2011.
28. Singh, D.D.; Sahoo, S.; Sharma, M.; John, S. Geospatial analysis of groundwater quality in Ludhiana, Punjab (India). *J. Geo. Environ. Earth Sci. Inter.* **2019**, *20*, 1–12. [CrossRef]
29. Census of India. District Hand Book; Ludhiana; Directorate of Census Operations; Punjab. 2011. Available online: http://censusindia.gov.in/2011census/dchb/0307_Part_B_DCHB_Ludhiana.pdf (accessed on 16 December 2018).
30. India Meteorological Department (IMD). *Rainfall Statistics of India: Report*; Hydromet Division; Report No. Esso/Imd/Hs/Rainfall Report/01(2018)/24; IMD: New Delhi, India, 2017.
31. India Meteorological Department (IMD). Extreme weather events of Ludhiana; Punjab. 2018. Available online: http://city.imd.gov.in/citywx/localwx.php (accessed on 14 January 2019).
32. Micro, Small and Medium Enterprise (MSME). State Industrial Profile of Punjab. 2015. Available online: http://www.msmedildh.gov.in/State%20Profile%20of%20Punjab%2015-16.pdf (accessed on 24 November 2018).

33. Central Ground Water Board (CGWB). (2013) Groundwater Information Booklet; Ludhiana District; Punjab. 2013. Available online: http://cgwb.gov.in/District_Profile/Punjab/Ludhiana.pdf (accessed on 28 November 2018).
34. American Public Health Association (APHA). *Standards Methods for the Examination of Water and Waste Water*, 23rd ed.; APHA: Washington, DC, USA, 2017.
35. Mohan, S.V.; Nithila, P.; Reddy, S.J. Estimation of heavy metals in drinking water and development of heavy metal pollution index. *J. Environ. Sci. Health Part A* **1996**, *31*, 283–289. [CrossRef]
36. Prasad, B.; Bose, J.M. Evaluation of heavy metal pollution index for surface and spring water near a limestone mining area of the lower Himalayas. *Environ. Geology* **2001**, *41*, 183–188. [CrossRef]
37. Cengiz, M.F.; Kilic, S.; Yalcin, F.; Kilic, M.; Yalcin, M.G. Evaluation of heavy metal risk potential in Bogacayi River water (Antalya, Turkey). *Environ. Monit. Assess.* **2017**, *189*, 248–259. [CrossRef] [PubMed]
38. Brraich, O.S.; Jangu, S. Evaluation of water quality pollution indices for heavy metal contamination monitoring in the water of Harike Wetland (Ramsar Site): India. *Inter. J. Scient. Res. Pub.* **2015**, *5*, 36–40.
39. Rezaei, A.; Hassani, H.; Jabbari, N. Evaluation of groundwater quality and assessment of pollution indices for heavy metals in North of Isfahan Province, Iran. *Sustain. Water Resour. Manag.* **2017**, *5*, 491–512. [CrossRef]
40. Shankar, B.S. A critical assay of heavy metal pollution index for the groundwater's of Peenya industrial area, Bangalore, India. *Environ. Monit. Assess.* **2019**, *191*, 289–302. [CrossRef] [PubMed]
41. Giri, S.; Singh, G.; Gupta, S.K.; Jha, V.N.; Tripathi, R.M. An evaluation of metal contamination in surface and groundwater around a proposed uranium mining site, Jharkhand, India. *Mine Water Environ.* **2010**, *29*, 225–234. [CrossRef]
42. Giri, S.; Singh, A.K. Human health risk assessment via drinking water pathway due to metal contamination in the groundwater of Subarnarekha River Basin, India. *Environ. Moint. Assess.* **2015**, *187*, 63–77. [CrossRef] [PubMed]
43. Tamasi, G.; Cini, R. Heavy metals in drinking waters from Mount Amiata (Tuscany, Italy). Possible risks from arsenic for public health in the province of Siena. *Sci. Total Environ.* **2004**, *327*, 41–51. [CrossRef] [PubMed]
44. United States Environmental Protection Agency (US EPA). *Risk Assessment Guidance for Superfund Volume 1 Human Health Evaluation Manual (Part A) Interim Final*; EPA/540/1-89/002; United States Environmental Protection Agency: Washington, DC, USA, 1989.
45. United States Environmental Protection Agency: Integrated Risk Information System (US EPA IRIS). *Reference Dose for Oral Exposure*; United States Environmental Protection Agency: Washington, DC, USA, 2011. Available online: http://cfpub.epa.gov/ncea/iris_drafts/atoz.cfm?list_type=alpha. (accessed on 15 January 2019).
46. Li, W.; Wang, M.; Liu, L.; Wang, H.; Yu, S. Groundwater heavy metal levels and associated human health risk in the North China Plain. *Arab. J. Geosci.* **2015**, *8*, 10389–10398. [CrossRef]
47. United States Environmental Protection Agency (US EPA). *Exposure Factors Handbook*; National Center for Environmental; EPA/600/R-090/052F; United States Environmental Protection Agency: Washington, DC, USA, 2011.
48. United States Environmental Protection Agency (US EPA). *Risk Assessment Guidance for Superfund Volume 1 Human Health Evaluation Manual; Development of Risk—Based Preliminary Remediation Goals (Part-B)*; United States Environmental Protection Agency: Washington, DC, USA, 2010.
49. United States Environmental Protection Agency (US EPA). *Risk Assessment Guidance for Superfund Volume 1 Human Health Evaluation Manual (Part E; Supplementary Guidance for Dermal Assessment) Final*; EPA/540/R/99/005; United States Environmental Protection Agency: Washington, DC, USA, 2004.
50. Bureau of Indian Standards (BIS). *Drinking Water-Specifications*; 2nd revision of IS 10500; BIS: New Delhi, India, 2012.
51. Bhutiani, R.; Kulkarni, D.B.; Khanna, D.R.; Gautam, A. Geochemical distribution and environmental risk assessment of heavy metals in groundwater of an industrial area and its surroundings, Haridwar, India. *Energy Ecol. Environ.* **2017**, *2*, 155–167. [CrossRef]
52. Kumar, P.J.S.; Delson, P.D.; Babu, P.T. Appraisal of heavy metals in groundwater in Chennai city using a HPI model. *Bull. Environ. Contam. Toxicol.* **2012**, *89*, 793–798. [CrossRef] [PubMed]
53. Hundal, H.S.; Kumar, R.; Singh, K.; Singh, D. Occurrence and geochemistry of arsenic in groundwater of Punjab, Northwest India. *Communications in Soil Sci. Plant Anal.* **2007**, *38*, 2257–2277. [CrossRef]
54. Ray, S.S.P.; Elango, L. *Deterioration of Groundwater Quality: Implications and Management. Hand Book of Water Governance: Challenges and Prospects*; Springer: Singapore, 2019; pp. 1–12. [CrossRef]

55. Brindha, K.; Elango, L. Impact of tanning industries on groundwater quality near a metropolitan city in India. *Water Resour. Manag.* **2012**, *26*, 1747–1761. [CrossRef]
56. Bhagure, G.R.; Mirgane, S.R. Heavy metal concentrations in groundwater and soils of Thane Region of Maharashtra, India. *Environ. Monit. Assess.* **2011**, *173*, 643–652. [CrossRef] [PubMed]
57. Suresh, G.; Ramasamy, V.; Meenakshisundaram, V.; Venkatachalapathy, R.; Ponnusamy, V. Influence of mineralogical and heavy metal composition on natural radionuclide concentrations in the river sediments. *Appl. Radiation Isotopes* **2011**, *69*, 1466–1474. [CrossRef] [PubMed]
58. Chai, L.Y.; Wang, Z.X.; Wang, Y.Y.; Yang, Z.H.; Wang, H.Y.; Wu, X. Ingestion risks of metals in groundwater based on TIN model and dose-response assessment: A case study in the Xiangjiang watershed, central-south China. *Sci. Total Environ.* **2010**, *408*, 3118–3124. [CrossRef] [PubMed]